x-P-T phase diagram for the γ-α transition in $Ce_{0.9-x}La_xTh_{0.1}$ alloys

J. M. Lawrence,* J. D. Thompson, Z. Fisk, and J. L. Smith
Center for Materials Science, Los Alamos National Laboratory, Los Alamos, New Mexico 87545

B. Batlogg
AT&T Bell Laboratories, Murray Hill, New Jersey 07974
(Received 19 September 1983)

We report the results of resistivity measurements on $Ce_{0.9-x}La_xTh_{0.1}$ alloys for $x=0.10$, 0.11, 0.14, and 0.17 in the temperature interval 4.2—300 K and for the pressure range 0—12 kbar. Using these results we have semiquantitatively determined the P-T phase boundary for the isomorphic γ-α phase transition for each concentration x. For $x=0.10$, 0.11, and 0.14 the transitions are continuous at zero pressure, first order for pressures within the interval $P_c^L(x)<P<P_c^u(x)$, and continuous for higher pressures $P>P_c^u(x)$. Hence, for these concentrations the phase boundaries terminate at two critical points. For $x=0.17$, all observed transitions are continuous. Hence, in x-P-T space the surface of first-order transitions terminates at a critical edge ($T_c(x)$, $P_c(x)$) such that, over an interval of x, $P_c(x)$ is double valued and such that there is a "critical inflection point." These unusual features can be understood qualitatively as following from very general Fermi-liquid properties of the cerium $4f$ electronic system, together with the dilution and negative-pressure effects of alloying with lanthanum. We show that this qualitative description is consistent with existing experimental data.

I. INTRODUCTION

In cerium metal the γ-α phase transition, which is an isomorphic lattice collapse between two fcc phases of substantially different density, has been the subject of numerous investigations over the years.[1,2] While it is generally acknowledged that the transition involves a change in the character of the $4f$ electrons, the nature of this transformation is still a matter of dispute. In older work it was assumed that the $4f$ occupation undergoes a large decrease and concomitantly the valence increases when the metal transforms from the γ to the α state; this is the "promotional model." Older theories emphasized the role of electron screening interactions (the Falicov model) and lattice coupling (due to the large size mismatch between f^0 and f^1 configurations) in driving the first-order transition. Recent experiments[3-5] indicate, however, that the magnitude of the valence change is much smaller than previously expected. This has led to a variety of proposals concerning the mechanism of the transformation. These include models which treat the transformation as a Mott transition between a local-moment phase and a paramagnetic $4f$ band phase,[6] models in which changes in the Kondo exchange energy are responsible for the differing properties of the two phases,[7] models which stress the dynamics of the screening of the $4f$ electrons by the conduction electrons,[8] and models which argue that already in the free cerium atom there exists a tendency towards formation of two f orbitals of differing atomic size.[9]

One point on which all these models are in agreement is that in the ground state of cerium metal (and of many nonmagnetic cerium intermetallics) the $4f$ electronic system can be described as a Fermi liquid.[1] This is manifest in enhanced Pauli paramagnetism and linear coefficients of specific heat. There is a high level of universality among compounds: The properties scale with a characteristic Fermi-liquid temperature T_{FL} which varies between compounds over a broad range (1—1000 K). While it is generally understood that in the Fermi liquid the $4f$ spin degrees of freedom are quenched in the Pauli paramagnetic state, the microscopic character of the Fermi liquid is a matter of considerable dispute.

The γ-α phase boundary of cerium metal is known to terminate in a critical point in the P-T plane.[2] Studies[10] in $Ce_{0.9-x}M_xTh_{0.1}$ alloys (where M represents a rare-earth solute and the thorium is added to prevent formation of the double hcp β phase) also reveal the existence of a critical point x_c, T_c at $P=0$ in the x-T plane. The case of $Ce_{0.9-x}La_xTh_{0.1}$ is shown in Fig. 1. For various thermodynamic quantities, the large discontinuities and hysteresis associated with the transitions progressively shrink as x increases until beyond $x_c=0.09$ only continuous transitions are observed as broadened S-shaped curves. From a detailed analysis of many such curves, the phase boundary shown in the inset of Fig. 1 was obtained.[10]

Recently, it was speculated[7] that if the cerium P-T phase boundary could be extended to the negative-pressure region, a second low-temperature critical point might be observed. Since it is known[10] that the transition temperatures of cerium alloys are strongly dependent on the size of the solute M, with small (large) solutes exerting positive (negative) "chemical pressure," it was suggested that the negative-pressure region could be realized by appropriate choice of solute. Following this lead, we found[11] that for the alloy $Ce_{0.8}La_{0.1}Th_{0.1}$ the γ-α boundary terminates in two critical points in the P-T plane. This represents, to the best of our knowledge, the only reported example of a material with a phase boundary terminating in two critical

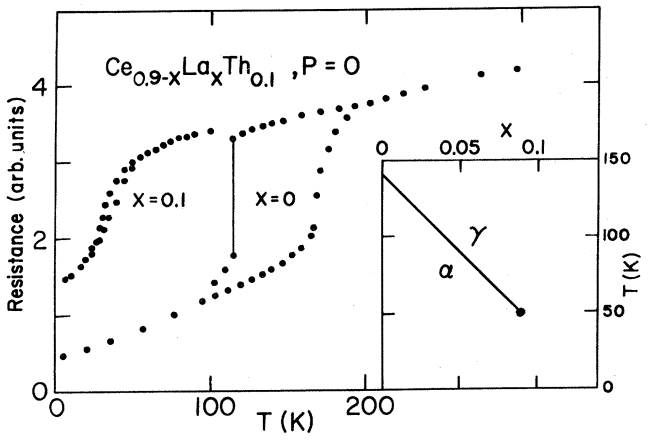

FIG. 1. Resistance vs temperature for $Ce_{0.9}Th_{0.1}$ and $Ce_{0.8}La_{0.1}Th_{0.1}$. The x-T,$P=0$ phase diagram for the γ-α transition in $Ce_{0.9-x}La_xTh_{0.1}$ is shown in the inset (from Ref. 10).

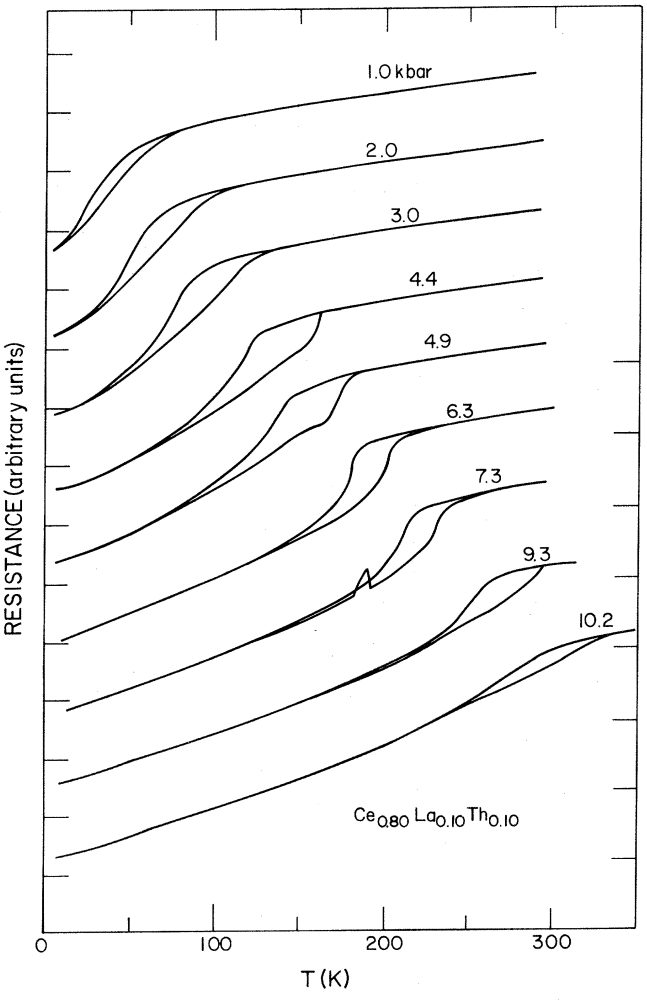

FIG. 2. Resistance vs temperature for $Ce_{0.80}La_{0.10}Th_{0.10}$ at several clamp pressures. The curves are displaced vertically for clarity.

points in the P-T plane. It is certainly related to a similar effect[1] occurring in the x-T plane of $Sm_{1-x}Y_xS$ alloys, which also exhibit an isomorphic valence transition, but the nature of the relationship is not entirely clear. (Similar phase boundaries are exhibited in the μ-T plane of certain binary mixtures that exhibit both an upper and lower consolute temperature.[12])

Here we report a more thorough study of the x-P-T phase diagram of $Ce_{0.9-x}La_xTh_{0.1}$ alloys. This allows a semiquantitative determination of the two-dimensional surface of first-order transitions in x-P-T space and its termination at a critical edge $(P_c(x),T_c(x))$. Over a certain range of concentrations $x_c(P=0)<x<x_I$, this edge is double valued so that, for fixed x, two critical points are observed on the γ-α boundary. At the concentration x_I, a "critical inflection point" occurs, and for larger x no first-order transitions are observed. We show that this unusually shaped phase diagram in x-P-T space can be understood qualitatively in terms of the above-mentioned very general Fermi-liquid behavior of the cerium $4f$ electronic system in the presence of the negative-pressure effects of lanthanum dilution. The transition is viewed as occurring between two states of differing characteristic Fermi-liquid temperature T_{FL}, with the nonlinear volume dependence of T_{FL} playing a crucial role. Existing data for T_{FL}, while not definitive, are consistent with this approach. While we make no pretense to pinpoint the microscopic character of the Fermi liquid, this approach does allow us to discuss the phase diagram (and its relationship to the phase diagrams of related materials) in a natural way.

The outline of the paper is as follows. In Sec. II we describe the experimental techniques. In Sec. III we present the results of studies of the pressure and temperature dependence of the resistivity of several alloys and we analyze these to determine the phase diagram. In Sec. IV we discuss the thermodynamics of the transition utilizing the Fermi-liquid approach. In Sec. V we discuss the assumptions underlying this treatment. We then consider recent calculations where the Fermi liquid is modeled as a Kondo system; in doing this we stress that the qualitative features of the phase diagram follow from very general properties which may be present in other microscopic models. We also consider in Sec. V the extension of these ideas to other $Ce_{1-x}M_x$ alloys as well as SmS alloys.

II. EXPERIMENTAL DETAILS

Rectilinear samples were cut from arc-melted buttons and their resistance was measured by a four-probe ac technique. The sample geometry was not adequate to allow a precise determination of the resistivity, and the changes in sample dimension through the transition, which is a 5% effect, have not been determined. Hence, we quote the results as resistance in arbitrary units. To give the reader an idea of the magnitudes involved, we estimate that the resistivity at room temperature for these samples is of order 70—80 $\mu\Omega$ cm.

For an isomorphic transition, the order parameter is the cell volume (or lattice constant). In earlier studies[13] of $Ce_{1-x}Th_x$, it was found that in the critical region the resistivity varies proportionately with the cell volume. To

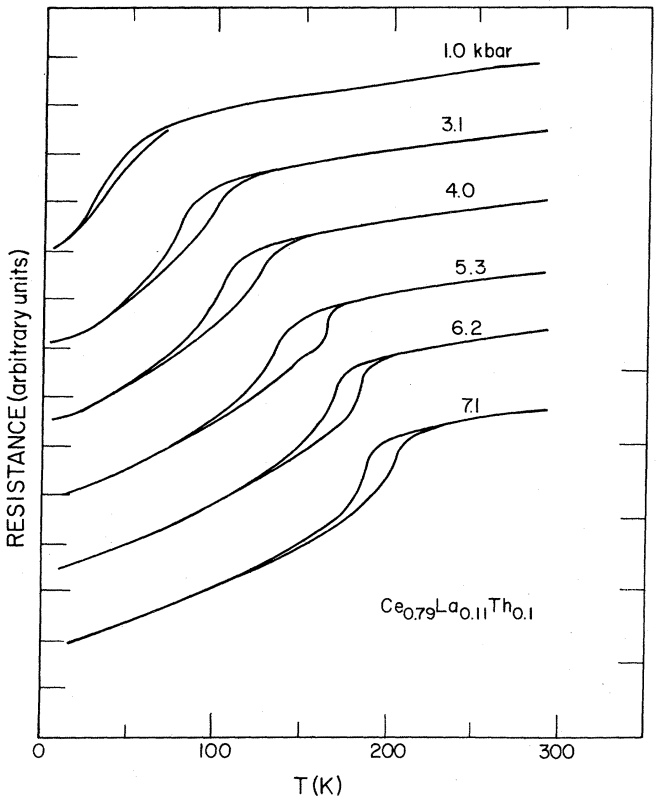

FIG. 3. Resistance vs temperature for $Ce_{0.79}La_{0.11}Th_{0.10}$ at several clamp pressures. The curves are displaced vertically for clarity.

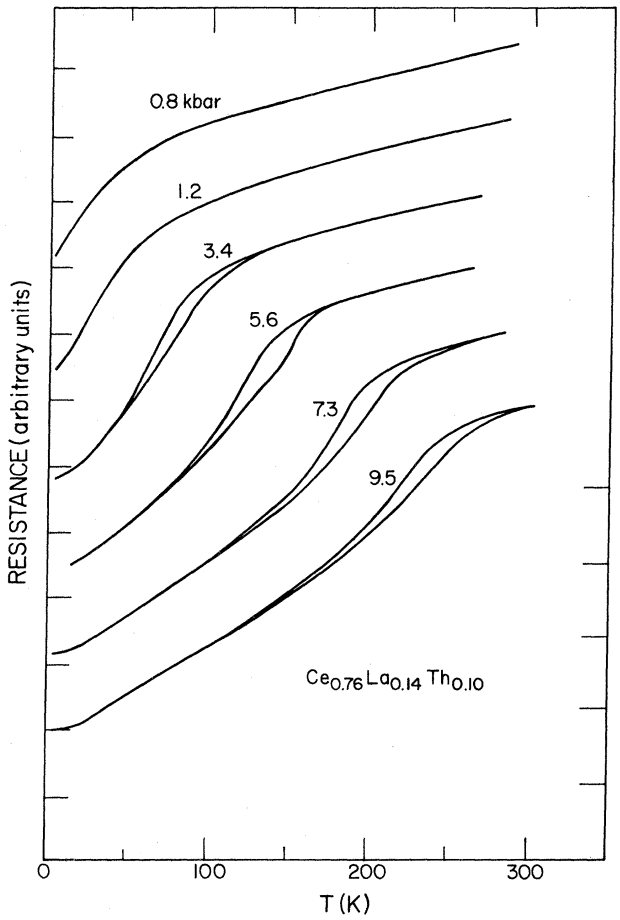

FIG. 4. Resistance vs temperature for $Ce_{0.76}La_{0.14}Th_{0.10}$ at several clamp pressures. Curves are displaced vertically for clarity.

the extent that this is so, our resistance curves may be thought of as representing the order parameter for the transition.

The samples were placed in a self-clamping cell, which was pressurized at room temperature. The pressure medium was a 1:1 mixture of *n*-pentane and isoamyl alcohol. The cell was lowered gradually into a helium bath with cooling rates kept small to avoid spurious hysteresis. The pressure was calibrated at low temperature by measuring inductively the superconducting transition temperature of a lead sample included in the cell. To measure the temperature dependence of the pressure in the cell, we measured the resistance of a manganin wire [whose $R(P)$ curve had been precalibrated at room temperature] at various press loads as a function of temperature.[14] With the assumption that the pressure derivative dR/dP of the manganin was independent of temperature, the cell pressure was obtained at all temperatures. At low temperatures the pressure so obtained was in excellent agreement with the value determined from the lead transition. Under conditions considered here, we found that the cell pressure is nearly constant up to 100 K and increases linearly at higher temperatures. The results shown in Figs. 2–5 were obtained at constant press load and are not corrected for the thermally induced pressure variation; the pressures quoted are those appropriate to the low-temperature region. The phase-transformation pressures given in Fig. 6 have been corrected for this effect.

A feature that is usually present in studies of cerium al-

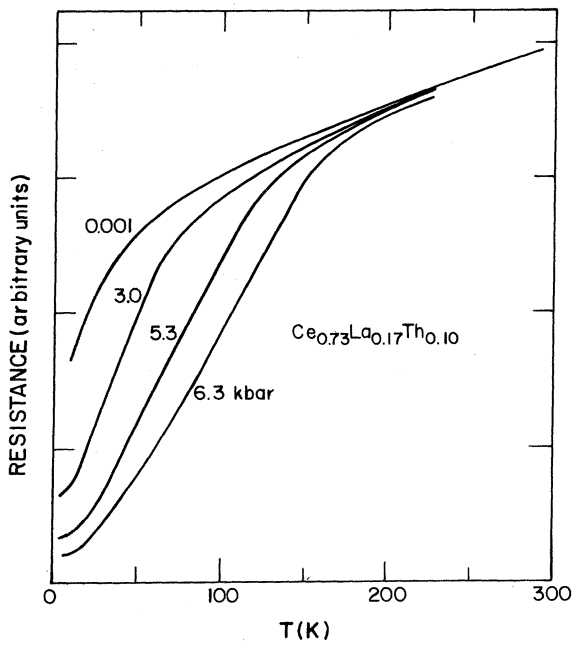

FIG. 5. Resistance vs temperature for $Ce_{0.73}La_{0.17}Th_{0.10}$ at several clamp pressures.

loys and which complicates the analysis is the existence of a small [(2—3)-K] residual hysteresis, even for samples that exhibit continuous transitions.[13] This can be seen for concentration $x=0.1$ in Fig. 1; a related effect is the rounding of the warming transition for $Ce_{0.9}Th_{0.1}$. This

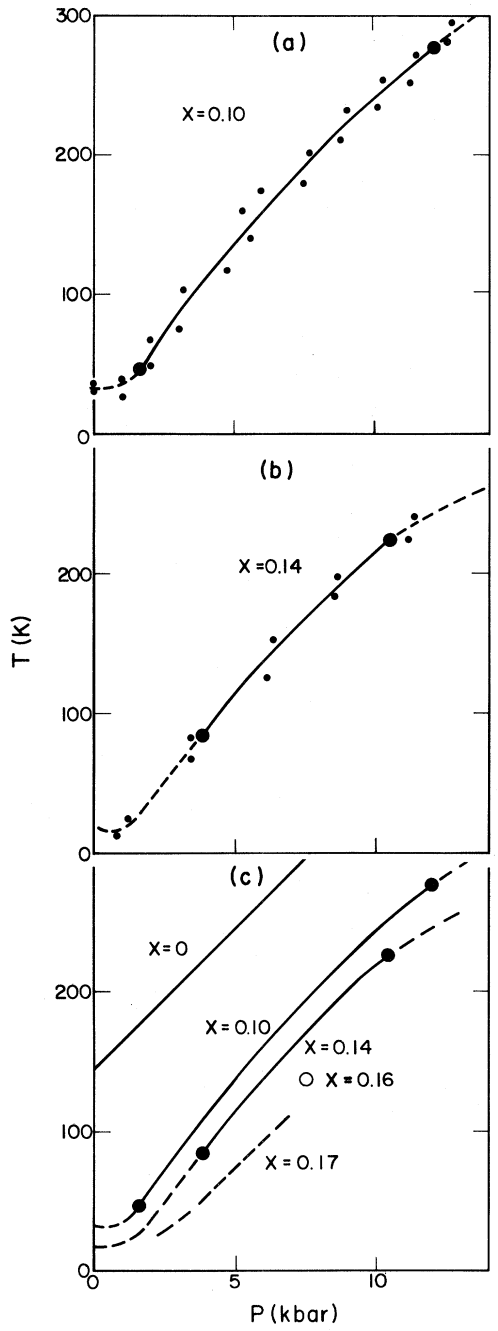

FIG. 6. Pressure-temperature phase diagrams for $Ce_{0.9-x}La_xTh_{0.1}$ with (a) $x=0.10$ and (b) $x=0.14$. The small solid circles give the values of P and T for the warming and cooling transitions, and the solid lines are our estimate of the equilibrium phase boundary of first-order transitions with their terminations in critical points (large solid circles). The dashed lines represent the locations of the continuous transitions. The equilibrium boundaries are plotted together in (c) together with the $x=0$ data from Ref. 15 and our $x=0.17$ data. The open circle in (c) gives our estimate of the parameters of the "critical inflection point."

can be understood as a manifestation of alloy inhomogeneity: For a distribution of concentrations x about the mean value $\bar{x}$, a certain fraction of the sample will exhibit hysteretic first-order transitions even when the transition for the mean value should be continuous. The inhomogeneous strain fields which are expected to accompany the enormous cell collapse ($\Delta V/V\sim 0.15$) can also contribute. These effects are compounded further in the high-pressure cell by the existence of small gradients in the pressure medium and by unavoidable pressure changes that occur when the sample volume changes within the frozen medium. Such effects are strongest in the vicinity of the critical points where the thermodynamic properties vary rapidly with x and P. Indeed, we found that for $x=0.14$ no hysteresis was observable at low pressures but appeared only as the pressure approached the pressure of the lower critical point; for $x=0.17$, no hysteresis was observed at any pressure below 7 kbar. Owing to this residual hysteresis we found that it was not possible to use the analysis developed for $Ce_{1-x}Th_x$ alloys[13] to determine precisely the parameters of the critical region. Hence, the phase boundaries given in Fig. 6 represent only a semiquantitative estimate based on the qualitative features of the data.

III. EXPERIMENTAL RESULTS

As can be seen from Fig. 1, for alloys of $Ce_{0.9-x}La_xTh_{0.1}$ with concentration x greater than the critical concentration $x_c=0.09$, the transitions are continuous. When pressure is applied to the alloy with a concentration ($x=0.10$) slightly larger than x_c, the following sequence is observed (Fig. 2). Below 2 kbar the transitions remain S shaped and continuous. At higher pressures the transitions are clearly first order: The hysteresis becomes enormous and the transitions (especially upon warming) appear discontinuous. These effects reach a maximum near 5 kbar. At the highest pressure the transition again appears S shaped and continuous. A very similar sequence is observed for $x=0.11$ (Fig. 3). For the concentration $x=0.14$, the sequence is qualitatively different (Fig. 4). At low pressures the "residual hysteresis" discussed in Sec. II is not observed; this is because the values of x and P are sufficiently different from the critical values that the alloy and pressure inhomogeneities are insufficient to allow any regions of the sample to have first-order transitions. At somewhat higher pressures (the curve marked 3.4 kbar in Fig. 4) residual hysteresis is observed, but the transition still appears to be continuous. For still higher pressures, the transition is markedly discontinuous (5.6 and 7.3 kbar); for the highest pressure studied, the transition is once again continuous. As shown in Fig. 5 for the largest concentration studied ($x=0.17$), there is a further qualitative change: No residual hysteresis is observed and all transitions are continuous up to 6.3 kbar.

In Figs. 6(a) and 6(b) we plot the transition temperatures estimated for warming and cooling for two of the samples (small solid circles). (We remind the reader that the pressures quoted here differ from those given in Figs. 2—4 in that they have been corrected for the temperature variation of the cell pressure.) As a result of the effects mentioned in Sec. II, the first-order transitions are sub-

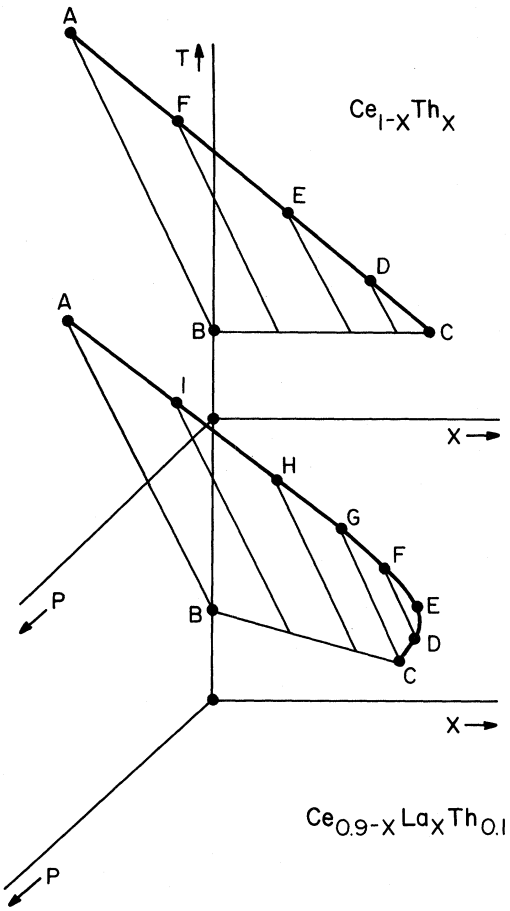

FIG. 7. Schematic representations of the x-P-T phase diagrams for $Ce_{1-x}Th_x$ and $Ce_{0.9-x}La_xTh_{0.1}$.

stantially rounded and it is difficult to precisely locate the critical points. Nevertheless, the actual phase boundaries for $x=0.10$, 0.11, and 0.14 clearly exhibit two critical points. In Figs. 6(a) and 6(b) we have estimated the location of the critical points on qualitative grounds and have drawn a smooth curve between the warming and cooling transitions as an estimate of the equilibrium phase boundary. The dashed lines represent the midpoints of the continuous transitions. In Fig. 6(c) we have replotted the estimated phase boundaries for $x=0.10$ and 0.14 along with the midpoints of the continuous transitions for $x=0.17$. In addition, we have included the low-temperature portion of the phase boundary for $Ce_{0.9}Th_{0.1}$ ($x=0$) as measured by Huang *et al.*[15] For this concentration there is no low-temperature critical point, and while the high-temperature critical point has not been located, a reasonable estimate would be $P_c=15$ kbar and $T_c=450$ K.

The following qualitative features are apparent from Fig. 6(c). Firstly, at fixed pressure, the transition temperatures decrease with increasing concentration x. Secondly, the pressure of the low-temperature critical point increases, while that of the high-temperature critical point decreases with increasing x. At some concentration x_I the two critical points should coalesce into one; beyond this concentration only continuous transitions would be observed. We estimate that the value of x_I is 0.16, so that the sample with $x=0.17$ would have only continuous transitions. The critical inflection point appears as a single small open circle in the P-T plane; we have plotted a reasonable estimate in Fig. 6(c) ($x_I=0.16$, $T=140$ K, and $P=7.5$ kbar).

These results are somewhat clearer when visualized in three dimensions. Qualitatively, the x-P-T phase diagram has the appearance shown in Fig. 7. Consider first the case $Ce_{0.9-x}La_xTh_{0.1}$. The line *BC* is the first-order boundary in the x-T plane at zero pressure, which terminates at the zero-pressure critical point $C(x_c(P=0),T_c(P=0))$ and the line *AB* is the phase boundary in the P-T plane for $x=0$ terminating at the critical point $A(P_c(x=0),T_c(x=0))$. The curve *AC* is a line of critical points (the "critical edge") which is the termination of a surface of first-order transitions. The points *F*, *G*, *H*, and *I* are high-temperature critical points, while *D* is a low-temperature critical point, and the point *E* is a "critical inflection point," corresponding to the concentration x_I beyond which the transitions are continuous. The line *DF* is a phase boundary at fixed x with two critical points. For all concentrations x in the interval $x_c(P=0)<x<x_I$, two critical points are observed. The shape of this is to be contrasted with the x-P-T phase diagram for $Ce_{1-x}Th_x$, at the top of Fig. 7. In that system, application of pressure to samples with x close to $x_c(P=0)$ always makes the transitions *less* first order.[15] The critical edge is nearly linear and $P_c(x)$ is single valued everywhere.

We stress once more that the phase boundaries given in Fig. 6 are only semiquantitative. Owing to the residual hysteresis effects discussed above, it is not possible to distinguish precisely between first- and second-order transitions. Our qualitative criterion is that transitions which are broad and S shaped with residual hysteresis of only a few degrees are second order (e.g., the transitions marked 1.0 and 10.2 kbar in Fig. 2), while transitions with large hysteresis and kinks or discontinuities (e.g., the transitions between 4 and 6 kbar in Figs. 2—4) are first order. Insofar as any one concentration x shows a lower and upper critical point, while some larger x shows only continuous transitions, the three-dimensional phase diagram *must* have the form shown in Fig. 7. That this is so is, we believe, amply demonstrated by our data. For example, if one were to insist that all curves showing hysteresis are first order, then the sample $x=0.14$ satisfies the former criterion and the sample $x=0.17$ satisfies the latter, so that the phase boundary of Fig. 7 holds but Fig. 6 would have to be revised. However, we wish to point out that in the presence of alloy and pressure inhomogeneity, residual hysteresis *must* be observed even where the mean concentration and pressure represents a continuous transition. Hence, we think the estimates given in Fig. 6 are not too inaccurate.

IV. THERMODYNAMICS OF THE TRANSITION IN A FERMI-LIQUID MODEL

To continue the discussion of the phase diagram, we consider the following free-energy functional appropriate to $Ce_{1-x}La_x$ alloys:[7,11]

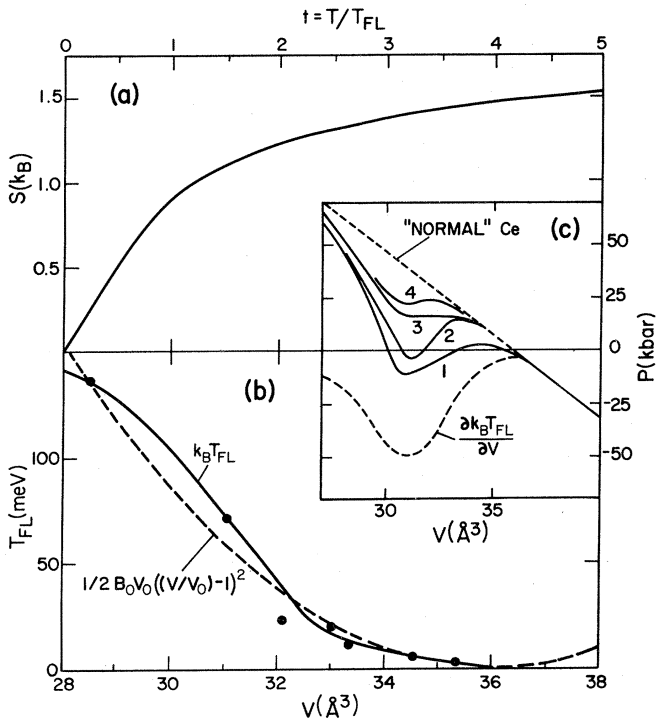

FIG. 8. (a) Entropy as a function of scaled temperature $t=T/T_{\rm FL}$ for cerium compounds. $T_{\rm FL}$ is the Fermi-liquid temperature. (b) Characteristic temperatures $T_{\rm FL}$ as a function of volume per atom for cerium alloys. The points are estimates of $T_{\rm FL}$ using inelastic-neutron-scattering linewidth data (Refs. 16 and 17). The smooth solid line is our interpolation. The dashed line is a plot of the first term on the right-hand side of Eq. (1c). (c) Dashed lines represent separately the sum of the normal P-V isotherm and the term $-\partial(k_B T_{\rm FL})/\partial V$. Curve 1 is the sum of these two terms. Curve 2 represents qualitatively the change in shape of the isotherm at low temperatures. Curve 3 represents a critical isotherm obtained from curve 1 by either raising the temperature or by alloying at $T=0$. Curve 4 represents the result of first alloying (so as to obtain curve 3 at $T=0$) and then raising the temperature.

$$G=(1-x)F^{\rm Ce}(V)+xF^{\rm La}(V)+PV\ , \tag{1a}$$

where

$$F^{\rm La}=\tfrac{1}{2}B_0^{\rm La}V_0^{\rm La}(V/V_0^{\rm La}-1)^2 \tag{1b}$$

and

$$F^{\rm Ce}=\tfrac{1}{2}B_0^{\rm Ce}V_0^{\rm Ce}(V/V_0^{\rm Ce}-1)^2+F_{\rm FL}(T;V)\ . \tag{1c}$$

Except for the last (Fermi-liquid) term in $F^{\rm Ce}$, the free energy is that of a simple mixture in the approximation that every atom in the alloy possesses the same average volume V. The "normal" volume dependence is calculated from the strain-energy penalty each component "pays" to adjust to the average volume V. The normal volume V_0 and bulk modulus B_0 for lanthanum are those appropriate for the pure fcc metal; for cerium they are taken as the values the trivalent metal would have in the absence of the anomalous terms, which can be obtained by smoothly interpolating between the values for lanthanum and praesodynium to be, respectively, 36 Å^3 and 280 kbar.

The anomalous terms driving the phase transition are represented as an energy $E_{\rm FL}(T;V)$ and entropy $S_{\rm FL}(T;V)$ of the $4f$ Fermi liquid. The transition is viewed as occurring between two states of very different characteristic temperatures, namely, $T_{\rm FL}\approx 1000$ K in the α state and $T_{\rm FL}\approx 100$ K in the γ state. (The evidence that this is so can be found in the inelastic-neutron-scattering spectra.[16,17]) The temperature dependence is determined by the entropy of the Fermi liquid. It is known from experimental studies in many cerium compounds that the thermodynamic properties scale with $T_{\rm FL}$;[18] this means that the entropy $S_{\rm FL}(t)$ is a universal function of scaled temperature $t=T/T_{\rm FL}$; i.e., $S_{\rm FL}(T;V)=S_{\rm FL}(T/T_{\rm FL}(V))$. When integrated, such an entropy yields a free energy of the form

$$F_{\rm FL}(T;V)=E_{\rm FL}^0(V)-Tf(T/T_{\rm FL}(V))\ , \tag{2a}$$

where

$$f(t)=\frac{1}{t}\int_0^t S(t')dt'\ . \tag{2b}$$

The condensation energy $E_{\rm FL}$ is expected to be of order $k_B T_{\rm FL}(V)$, which experimentally is known[7] to be a strongly nonlinear function of the cell volume. Hence, from this point of view the primary nonlinearity, which allows for first-order transitions, arises from the volume dependence of the characteristic energy $k_B T_{\rm FL}$.

Let us first consider the situation for pure cerium. The equilibrium volume at fixed T and P is given by

$$0=\frac{\partial G}{\partial V}=P+\frac{B_0^{\rm Ce}}{V_0^{\rm Ce}}(V-V_0^{\rm Ce})+\frac{\partial E_{\rm FL}^0}{\partial V}+\frac{T^2 f'_{\rm FL}}{T_{\rm FL}^2}\frac{\partial T_{\rm FL}}{\partial V}\ , \tag{3}$$

where the prime indicates differentiation of $f(t)$ with respect to the scale variable t. First-order transitions will occur in the region where $V(P)$ is multivalued; and the solid will be unstable for negative values of the bulk modulus $B=-V\partial P/\partial V$. To explore this possibility we need to consider the temperature dependence of $S_{\rm FL}$ and the volume dependence of $T_{\rm FL}$. To estimate the entropy we proceed as follows: It is known from theoretical studies[19] that the "effective moment" $T\chi/C$ (where χ is the susceptibility and C is the $J=\frac{5}{2}$ Curie constant) has nearly the same temperature dependence as the entropy. The effective moment has been shown to be a universal function of $T/T_{\rm FL}$ for cerium compounds.[18,20] For the sake of discussion we assume $S/k_B\ln 6\equiv T\chi/C$ and plot the experimentally determined value in Fig. 8(a). We next make the assumption that $E_{\rm FL}^0\equiv -k_B T_{\rm FL}$ which, while not exact, should be correct within an order of magnitude and simplifies the discussion. In Fig. 8(b) we plot the volume dependence of the linewidths measured in inelastic-neutron-scattering spectra for certain alloys;[16,17] this is a standard measure of $T_{\rm FL}$. In addition, we plot there the normal volume dependence of $F^{\rm Ce}$ with normal bulk modulus $B_0^{\rm Ce}=280$ kbar. The P-V relation at $T=0$ can be found by summing the derivatives of these latter two terms. To accomplish this we have somewhat arbitrarily drawn a smooth curve through the data points for $k_B T_{\rm FL}$ and differentiated numerically. The results are shown in Fig. 8(c). Curve 1 is the P-V relation so determined for pure cerium at $T=0$. This exhibits the essential feature that as the pressure increases from large negative values there is a first-order transition from the high-volume state

to the low-volume state occurring in the negative-pressure region. If we assume these have volumes of order 36 and 30 Å^3, respectively, then by equating the free energies in the two states and utilizing Fig. 8(b) to determine E_{FL}, we obtain $P_0(T=0)\approx -5$ kbar.

Next we consider the situation for pure cerium at fixed pressure ($P=0$). At $T=0$ the system will be in the low-volume state. As the temperature increases, the large entropy gain will lower the free energy of the γ state until at some temperature $T_0(P=0)$ there will be a first-order transition to the high-volume state. Assuming the same values of V_γ and V_α as above and an entropy gain of $1.5k_B$, the Clausius-Clapyron equation yields $\Delta P/\Delta T=30$ K/kbar and $T_0(P=0)=150$ K, in good agreement with experiment.[2]

As the temperature increases, there is a significant effect on the shape of the P-V isotherm. As T increases, the final term in Eq. (3) increases the pressure at fixed V; since the magnitude of the increase varies as $[T/T_{FL}(V)]^2$, the effect is biggest at high volumes where T_{FL} is smallest. The net effect is shown qualitatively as curve 2 in Fig. 8(c); the P-V curve becomes more nonlinear (and the transitions more strongly first order) as T initially increases. At very high temperatures, where the entropy saturates to $k_B\ln 6$, the isotherm will become monotonic. The temperature at which the isotherms change from multiple valued to monotonic is, of course, that of the high-temperature critical point; the critical isotherm is shown qualitatively as curve 3.

For the alloy case, we have

$$P=(1-x)P^{Ce}(V)+x\frac{B_0^{La}}{V_0^{La}}(V_0^{Ce}-V)+x\frac{B_0^{La}}{V_0^{La}}(V_0^{La}-V_0^{Ce}), \tag{4}$$

where $P^{Ce}(V)$ is the P-V relation for pure cerium, Eq. (3). Alloying has two main effects. The final term in Eq. (4) acts as a constant-pressure shift so that part of the negative-pressure region of Fig. 8 becomes accessible at positive pressure. (For $V_0^{La}=37.5$ Å^3 and $B_0^{La}=279$ kbar, the magnitude of this shift is 1 kbar for $x=0.1$). The second effect is that the Fermi-liquid terms are diluted, i.e., the contribution of the term $-\partial(k_BT_{FL})/\partial V$ to the isotherm decreases with increasing x. There will be a critical concentration $x_C(T=0)$ such that the $T=0$ isotherms will be single valued for larger concentrations. However, it remains that as temperature initially increases the P-V isotherms become more nonlinear and first order-like. Hence, for a concentration x slightly larger than $x_C(T=0)$, the $T=0$ isotherm will qualitatively resemble curve 3 of Fig. 8(c), but the isotherm at slightly elevated temperature will resemble curve 4. This leads to a lower critical point on a P-T phase diagram which will occur at positive pressure, if the constant-pressure shift mentioned above is large enough. As the temperature is raised still further, the entropy terms again will saturate and the isotherms approach that of the normal material, leading to a second (upper) critical point. However, for a sufficiently large concentration $x>x_I$, the Fermi-liquid terms will be diluted so strongly that only continuous transitions are possible at any temperature. The concentration x_I is then that of the critical inflection point.

V. DISCUSSION

We have seen that the experimental x-P-T phase diagram shown in Figs. 6 and 7 has a qualitative explanation in terms of a free-energy functional which includes the Fermi-liquid behavior in a natural way. First-order transitions occur because the condensation energy is a highly nonlinear, decreasing function of volume. The main tendency of alloying is to dilute the Fermi-liquid terms and hence make the transitions continuous. However, because the Fermi-liquid entropy develops more rapidly with temperature at larger V, the P-V isotherms tend to become more first order as T initially increases. Over a limited range of x this leads to P-T phase boundaries with two critical points.

This treatment, while qualitative, is not tied to any specific microscopic model but is cast in terms of the experimentally established Fermi-liquid behavior. In this section we discuss several of the assumptions which were made in the course of the treatment. Following this we discuss the relation of our general treatment to a recent calculation[7,11] of the cerium phase diagram. Finally, we discuss the possibility of realizing similar phase diagrams in other alloy systems.

A. Assumptions underlying the Fermi-liquid treatment

The free-energy functional [Eq. (1)] does not include the energy or entropy of mixing of the alloy. This we justify on the basis that diffusion is limited in the low-temperature solid, so that the concentration x (as opposed to the chemical potential) becomes a constrained variable, i.e., the free energy of mixing will be only a weakly varying function of temperature. Secondly, we have calculated the normal volume dependence in the harmonic approximation, under the assumption that the normal contribution to the thermal expansion (typically 10^{-5}/K) is a small fraction of the volume expansion at the phase transition ($\Delta V/V\simeq 0.1$). Thirdly, we have neglected to discuss the role of thorium dilution. This will have a comparable effect to lanthanum in diluting the nonlinear Fermi-liquid terms but will have a different effect on the absolute value of the pressure at the transition. On the basis of size alone, addition of thorium acts as positive chemical pressure (where lanthanum dilution gives negative chemical pressure). However, it is known experimentally[10] that there is also a valency effect (i.e., trivalent solutes such as lanthanum stabilize the γ state more strongly than thorium, which is tetravalent) which should be included in a more complete treatment.

The assumption that the entropy is proportional to the effective moment ($S/k_B\ln 6=T\chi/C$) is more in the nature of a convenience for the sake of discussion. What is clear experimentally is that the entropy is qualitatively as shown in Fig. 8(a): linear at low temperatures, saturating to the free-ion value for $T\gg T_{FL}$, and scaling with T/T_{FL}. For example, the ratio of the effective moment to the low-temperature linear specific heat has essentially the free-Fermi-gas value for most cerium compounds.[18,21]

The most serious assumption is that the ground-state energy E_{FL}^0 can be identified as $-k_BT_{FL}$. This cannot be justified on the basis of experiment alone. However, it

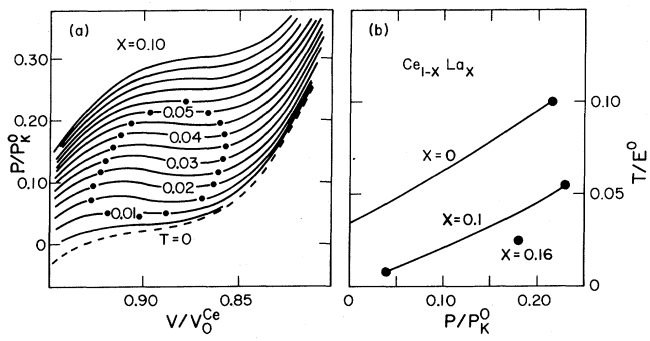

FIG. 9. *P-V* isotherms and *P-T* phase boundaries for $Ce_{1-x}La_x$ alloys as calculated in a model where the Fermi-liquid free energy is taken from the solution of the spin-$\frac{1}{2}$ Kondo problem. The units are $V_0=36$ Å^3, $P_k^0=34$ kbar, and $T=0.04$ corresponds to 300 K (from Ref. 11).

does appear to be a feature of certain theories of valence fluctuation effects. For example, in a Kondo model it appears to hold for large orbital degeneracy, while for the spin-$\frac{1}{2}$ case, strict proportionality does not hold.[22] For the sake of the qualitative discussion, the essential requirement is merely that E_{FL} be a strongly nonlinear, decreasing function of volume; this is valid even for the spin-$\frac{1}{2}$ case.

Once these assumptions are made, it becomes possible to *calculate* the *P-V* isotherms at all T from experimental data alone. In our qualitative treatment, we somewhat arbitrarily drew a smooth curve through the data for $k_BT_{FL}(V)$ and differentiated graphically. Given the error bars and the limited amount of available data, it would be quite possible to draw this curve with smaller slope in the region of interest so that the minimum in $\partial(k_BT_{FL})/\partial V$ would be substantially shallower, thereby altering the phase diagram in significant ways. To resolve this difficulty requires more data for $k_BT_{FL}(V)$. The appropriate experiment would be to measure the low-temperature value of the inelastic-neutron-scattering linewidths as a function of pressure in a $Ce_{0.8}La_{0.1}Th_{0.1}$ alloy, where T_{FL} can be scanned over most of the relevant range.

Given this uncertainty in the details of $T_{FL}(V)$, we can claim only that the Fermi-liquid treatment of the phase transition is consistent with the existing data. It is also consistent with a recent calculation[7] where the Fermi liquid was given an explicit microscopic model. What we are attempting here is to clarify the general features required of such a model that will yield the observed phase diagram.

B. Relation to recent calculations in a Kondo model

Recently, Allen and Martin[7] calculated the phase diagram for cerium metal by treating the system as a set of spin-$\frac{1}{2}$ Kondo impurities. This allows explicit calculation of the Fermi-liquid free energy for fixed Kondo coupling constant J. The dependence of J on volume was parametrized from experimental data, such as given in Fig. 8(b). The scaling property of the free energy is obeyed rigorously in this model. For the spin-$\frac{1}{2}$ case, the condensation energy varies as J^3, while the characteristic temperature varies as $\exp(-1/J)$; hence, T_{FL} is not rigorously proportional to E_{FL}^0. Nevertheless, the calculation agrees fairly well with the experimental phase diagram. More recently,[11] the calculation was extended to the alloy case; the results for $Ce_{1-x}La_x$ are shown in Fig. 9. (The calculation did not include terms for the thorium atoms; rather, it adjusted the parameters for the pure-cerium case to fit the properties of $Ce_{0.9}Th_{0.1}$.) The isotherms exhibit explicitly the sequence described above for the situation $x \gtrsim x_C(T=0)$, and the phase diagram is in good agreement with the experimental one shown in Fig. 6(c).

The restriction to spin-$\frac{1}{2}$ case is not necessary, as Bethe-ansatz solutions for the $J=\frac{5}{2}$ case now exist.[19] This should cause quantitative but not qualitative differences (e.g., in the relationship between E_{FL}^0 and k_BT_{FL}). A lesser known factor is the degree to which coherence between $4f$ electrons on neighboring sites will affect the calculation. Recent work[23] suggests that such coherence vanishes as $1/(2J+1)$ for large orbital degeneracy, but $J=\frac{5}{2}$ is probably an intermediate case. A deficiency of the calculation is that there is no microscopic justification given for the volume dependence of the coupling constant. However, since the coupling constant J depends on the hybridization matrix element[7] and since the latter is believed to be strongly volume dependent,[24,25] it is reasonable to argue that J varies strongly with volume (as $1/V^m$, $4 \lesssim m \lesssim 6$). The qualitative aspects of the phase diagram follow from such general properties of the Fermi liquid that it is possible that any of a number of other microscopic models[6,8,9] for cerium might duplicate the results. (Although, whether or not the other models *can* do this is not known *a priori*.) Hence, the microscopic character of the Fermi liquid cannot be resolved by the phase-diagram data alone.

C. Application to other alloys

Similar *x-P-T* phase diagrams can be expected in other $Ce_{1-x}M_x$ alloys. However, we have already mentioned that for $Ce_{1-x}Th_x$ alloys the application of pressure always makes the transitions more continuous;[15] hence, the *x-P-T* phase diagram has the appearance of Fig. 7 and there is no range of x where two critical points are observed. In terms of Fig. 8, the reason for this is that the transitions occur at temperatures which are already sufficiently elevated that they are above the range where the initial sharpening of the isotherms occurs. This, in turn, results from the fact that both the smaller size and larger valence of thorium relative to lanthanum favor stabilization of the low-volume state. The most likely cases for giving two critical points are then $M=$Yb and Eu, both of which are divalent and have larger atomic size than lanthanum. It is also possible that dilution with other trivalent rare earths, such as Pr or Gd, will create a comparable phase diagram as in the lanthanum case.

Finally, we consider the case of $Sm_{1-x}M_xS$ alloys. For $M=$Y and Gd, it is known[1] that the *x-T* phase diagram terminates in both an upper and a lower critical point. In terms of the free-energy functional [Eq. (1)], the lower critical point can be expected on the basis of the dilution

effect on the nonlinear terms alone. Experimentally, it is not known whether two critical points exist in any P-T plane at fixed x. An important difference to the cerium case is that the ground state for small x is not a Fermi liquid but rather a divalent $J=0$ singlet, and so the high-entropy state is the low-volume phase. This makes it difficult to generalize from the present results to the case of SmS.

ACKNOWLEDGMENTS

We are grateful to R. M. Martin for many useful discussions and to R. D. Parks for providing one of the samples. We also thank K. C. Lim and J. O. Willis for assistance in automating the data acquisition. The work at Los Alamos National Laboratory was performed under the auspices of the U. S. Department of Energy.

*Permanent address: Physics Department, University of California, Irvine, CA 92717.

[1]J. M. Lawrence, P. S. Riseborough, and R. D. Parks, Rep. Prog. Phys. 44, 1 (1981).

[2]D. C. Koskenmaki and K. A. Gschneidner, in *Handbook on the Physics and Chemistry of the Rare Earths,* edited by K. A. Gschneidner and L. Eyring (North-Holland, Amsterdam, 1978), Vol. 1, Chap. 4.

[3]R. D. Parks, N. Martensson, and B. Reihl, in *Valence Instabilities,* edited by P. Wachter (North-Holland, Amsterdam, 1982), p. 239.

[4]V. Kornstadt, R. Lasser, and B. Lengeler, Phys. Rev. B 21, 1898 (1980).

[5]B. Lengeler, G. Materlik, and J. E. Muller, Phys. Rev. B 28, 2276 (1983).

[6]B. Johansson, Philos. Mag. 30, 469 (1974).

[7]J. W. Allen and R. M. Martin, Phys. Rev. Lett. 49, 1106 (1982).

[8]S. H. Liu and K. M. Ho, Phys. Rev. B 26, 7052 (1982).

[9]M. Schlüter and C. M. Varma, in *Valence Instabilities,* Ref. 3; M. Schlüter and C. M. Varma, Bull. Am. Phys. Soc. 28, 341 (1983).

[10]M. A. Manheimer and R. D. Parks, Phys. Rev. Lett. 42, 321 (1979).

[11]J. D. Thompson, Z. Fisk, J. M. Lawrence, J. L. Smith, and R. M. Martin, Phys. Rev. Lett. 50, 1081 (1983).

[12]J. C. Wheeler and G. R. Andersen, J. Chem. Phys. 73, 5778 (1980); J. C. Wheeler and P. Pfeuty, J. Chem. Phys. 74, 6415 (1981).

[13]J. M. Lawrence, M. C. Croft, and R. D. Parks, Phys. Rev. Lett. 35, 289 (1975); J. M. Lawrence, Ph.D. thesis, University of Rochester, 1976; J. M. Lawrence, M. C. Croft, and R. D. Parks, in *Valence Instabilities and Related Narrow-Band Phenomena,* edited by R. D. Parks (Plenum, New York, 1977), p. 35.

[14]J. D. Thompson, Rev. Sci. Instrum. (to be published).

[15]C. Y. Huang, J. L. Smith, C. W. Chu, and P. H. Schmidt, in *High Pressure and Low Temperature Physics,* edtied by C. W. Chu and J. A. Wollam (Plenum, New York, 1978), p. 169; see also Sec. 2.1.1.3 of Ref. 1.

[16]S. M. Shapiro, J. D. Axe, R. J. Birgeneau, J. M. Lawrence, and R. D. Parks, Phys. Rev. B 16, 2225 (1977).

[17]B. H. Grier, R. D. Parks, S. M. Shapiro, and C. F. Majkrzak, Phys. Rev. B 24, 6242 (1981).

[18]J. M. Lawrence and M. T. Beal-Monod, in *Valence Fluctuations in Solids,* edited by L. M. Falicov, W. Hanke, and M. B. Maple (North-Holland, New York, 1981), p. 53.

[19]N. Andrei, K. Furuya, and J. H. Lowenstein, Rev. Mod. Phys. 55, 331 (1983); V. T. Rajan, Phys. Rev. Lett. 51, 308 (1983).

[20]J. M. Lawrence, Phys. Rev. B 20, 3770 (1979).

[21]D. M. Newns and A. C. Hewson, J. Phys. F 10, 2429 (1980).

[22]R. M. Martin (private communication).

[23]N. Read, D. M. Newns, and S. Doniach, Phys. Rev. Lett. (in press).

[24]W. A. Harrison and S. Froyen, Phys. Rev. B 21, 3214 (1980).

[25]O. K. Andersen, W. Klose, and H. Nohl, Phys. Rev. B 17, 1209 (1978); see Eq. (15).